

Experimental study of the polyamorphism of water. I. The isobaric transitions from amorphous ices to LDA at 4 MPa

Philip H. Handle, and Thomas Loerting

Citation: *The Journal of Chemical Physics* **148**, 124508 (2018); doi: 10.1063/1.5019413

View online: <https://doi.org/10.1063/1.5019413>

View Table of Contents: <http://aip.scitation.org/toc/jcp/148/12>

Published by the [American Institute of Physics](#)

Articles you may be interested in

[Experimental study of the polyamorphism of water. II. The isobaric transitions between HDA and VHDA at intermediate and high pressures](#)

The Journal of Chemical Physics **148**, 124509 (2018); 10.1063/1.5019414

[Equilibration and analysis of first-principles molecular dynamics simulations of water](#)

The Journal of Chemical Physics **148**, 124501 (2018); 10.1063/1.5018116

[Microscopic structural descriptor of liquid water](#)

The Journal of Chemical Physics **148**, 124503 (2018); 10.1063/1.5024565

[Comment on "The putative liquid-liquid transition is a liquid-solid transition in atomistic models of water" \[I and II: *J. Chem. Phys.* 135, 134503 \(2011\); *J. Chem. Phys.* 138, 214504 \(2013\)\]](#)

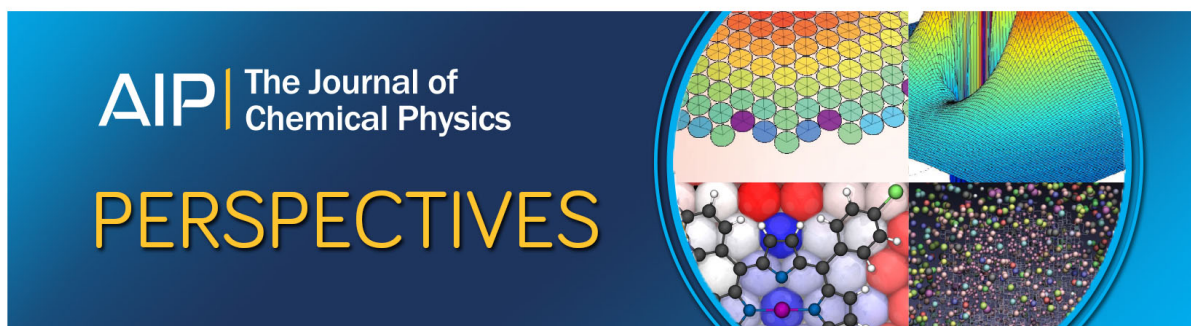
The Journal of Chemical Physics **148**, 137101 (2018); 10.1063/1.5029463

[The barrier to ice nucleation in monatomic water](#)

The Journal of Chemical Physics **148**, 124505 (2018); 10.1063/1.5016518

[Potential energy landscape of TIP4P/2005 water](#)

The Journal of Chemical Physics **148**, 134505 (2018); 10.1063/1.5023894



Experimental study of the polyamorphism of water. I. The isobaric transitions from amorphous ices to LDA at 4 MPa

Philip H. Handle^{a)} and Thomas Loerting^{b)}

Institute of Physical Chemistry, University of Innsbruck, Innrain 52c, A-6020 Innsbruck, Austria

(Received 14 December 2017; accepted 27 February 2018; published online 30 March 2018)

The existence of more than one solid amorphous state of water is an extraordinary feature. Since polyamorphism might be connected to the liquid-liquid critical point hypothesis, it is particularly important to study the relations amongst the different amorphous ices. Here we study the polyamorphic transformations of several high pressure amorphous ices to low-density amorphous ice (LDA) at 4 MPa by isobaric heating utilising *in situ* volumetry and *ex situ* X-ray diffraction. We find that very-high density amorphous ice (VHDA) and unannealed high density amorphous ice (HDA) show significant relaxation before transforming to LDA, whereby VHDA is seen to relax toward HDA. By contrast, expanded HDA shows almost no relaxation prior to the transformation. The transition to LDA itself obeys criteria for a first-order-like transition in all cases. In the case of VHDA, even macroscopic phase separation is observed. These findings suggest that HDA and LDA are two clearly distinct polyamorphs. We further present evidence that HDA reaches the metastable equilibrium at 140 K and 0.1 GPa but only comes close to that at 140 K and 0.2 GPa. The most important is the path independence of the amorphous phase reached at 140 K and 0.1 GPa. © 2018 Author(s). All article content, except where otherwise noted, is licensed under a Creative Commons Attribution (CC BY) license (<http://creativecommons.org/licenses/by/4.0/>). <https://doi.org/10.1063/1.5019413>

I. INTRODUCTION

A. Polyamorphism

Despite having a rather simple stoichiometry (H₂O), water is not a simple liquid. It displays complex behaviour and is often referred to as an anomalous liquid. This complexity fuels ongoing scientific interest as manifested in a recent thematic issue of *Chemical Reviews* titled “Water—The Most Anomalous Liquid.”¹ One popular attempt to explain the behaviour of water is the hypothesis of a liquid-liquid phase separation and an associated liquid-liquid critical point (LLCP) at temperatures far below the melting temperature.^{2–6} For the ST2 model of water,⁷ numerical studies indicate such a scenario.^{8–10} Also for TIP4P/2005,¹¹ a more recent and well performing model of water,¹² the existence of a LLCP is discussed.^{13–19} An experimental proof for this scenario is, however, missing even though indirect evidence for a LLCP at ≈50 MPa and ≈225 K is provided by Mishima *et al.*^{20–22} The difficulty in studying liquid water at temperatures far below the melting temperature is rapid crystallization,²³ rendering the interesting temperature interval practically impenetrable. Extremely high cooling rates of 10⁷ K s⁻¹ are required to beat crystallization at ambient pressure^{24–26} and somewhat less at elevated pressure.²⁷ Indirect evidence for a LLCP could however be provided by the study of the amorphous ices. If water really splits into

different liquids at low temperatures and if those liquids vitrify at even lower temperatures, clearly distinct glasses should be formed. This phenomenon, known as polyamorphism—a term to our knowledge first proposed by Wolf (cf. Ref. 28)—indicates the possibility for a substance to exist in more than one distinct amorphous “phase.” The identification of those forms with distinct polyamorphs would support the existence of distinct liquid phases in supercooled water. Recently, evidence for the diffusive nature of amorphous ices above their two distinct glass transition temperatures was presented,^{29–31} indicating them to be indeed in the ultraviscous liquid state.

A truly distinct polyamorph is characterized in that it can be formed utilising several different thermodynamic paths, and there is a sudden change of properties (e.g., density, expansivity) upon transformation to another polyamorph. One further necessity is the possibility to switch back and forth between different polyamorphs by pressure-cycling. Since this behaviour resembles first-order phase transitions, the terminology of phase transitions is used also for amorphous ices, in spite of their inherent non-equilibrium nature and in spite of the metastability with respect to crystalline ice. In order to account for the non-equilibrium character and metastability, transitions between amorphous ices are denoted first-order-like rather than first-order even though the stable phase can be avoided completely and quasi-equilibrium transformations between two phases of amorphous ice are possible.^{32,33} A precondition is that the relaxation in the metastable state is substantially faster than the time it takes for the metastable state to transform to a more stable phase (cf. Ref. 17). The fact

^{a)}Present address: Department of Physics, Sapienza University of Rome, Piazzale Aldo Moro 5, I-00185 Roma, Italy.

^{b)}Author to whom correspondence should be addressed: thomas.loerting@uibk.ac.at

that this condition is indeed met in amorphous ices was very recently shown.³⁴

Before we discuss the polyamorphism of water in more detail, a word of warning has to be uttered. From the non-equilibrium nature of amorphous systems follows that each thermodynamic path leads to a unique state. Therefore, the precise protocol of sample preparation becomes relevant. In order to systematize several coarsely related thermodynamic paths, abbreviations have been put forward to roughly categorize the thermodynamic history of the resulting samples. An amorphous ice bearing its own abbreviation does however not entail this form being a distinct polyamorph, i.e., a state that experiences a phase transition to other amorphous states. It just expresses that a specific thermodynamic path was followed during its production. The relation to other amorphous forms has to be studied carefully to determine which paths lead to truly different polyamorphs and which paths lead to variations of the same polyamorph.

B. Typical routes to amorphous ice

Having clarified that, we now turn to the different amorphous ices and their relations. Commonly encountered amorphous ices are low-density amorphous ice [LDA; $\rho(1 \text{ bar}) = 0.94 \text{ g cm}^3$], high-density amorphous ice [HDA; $\rho(1 \text{ bar}) = 1.15 \text{ g cm}^3$], and very high-density amorphous ice [VHDA; $\rho(1 \text{ bar}) = 1.26 \text{ g cm}^3$] as well as variations of those forms (density values taken from Ref. 35). HDA is usually produced by isothermally compressing hexagonal ice at 77 K to pressures exceeding 1.0 GPa.³⁶ This process is called pressure-induced amorphisation (PIA), and it is characterized by a rather sharp densification step forming the amorphous ice. If HDA is heated at pressures lower than $\approx 0.1 \text{ GPa}$, it transforms to LDA.^{32,36,37} If heated above $\approx 0.8 \text{ GPa}$, it transforms to VHDA³⁸ and it remains HDA if heated at pressures between ≈ 0.1 and $\approx 0.8 \text{ GPa}$.³⁹

Certain substates of HDA are further distinguished, namely, unannealed HDA (uHDA), being the HDA produced via PIA at 77 K, and expanded HDA (eHDA). The latter form is obtained by annealing uHDA at pressures below 0.5 GPa, which results in a decrease of density.⁴⁰ A different route to eHDA involves the decompression of VHDA at 140 K to pressures below 0.4 GPa.⁴¹ The exceptional property of eHDA is its transition temperature to LDA at 1 bar, for it is roughly 20 K higher than the one of uHDA.^{33,40,42} A similar effect on the transition temperature was also found when PIA was performed at temperatures significantly above 77 K.⁴³

Thus, three large categories of amorphous ices can be distinguished: LDA, HDA, and VHDA, where uHDA and eHDA are substates of the HDA category. This distinction in three large categories based on density suggests those forms to be candidates for different polyamorphs. Since this article is devoted to the relations of HDA and LDA as well as VHDA and LDA, we largely omit the discussion of the relation between VHDA and HDA. This latter relation, however, is the topic of Paper II⁴⁴ and hence discussed in detail there.

C. The relation between HDA and LDA

When the transition between HDA and LDA was first observed, the large and rapid change of density immediately suggested a first-order-like transition.^{36,37} Thermodynamic considerations even led to an estimation of the corresponding binodal⁴⁵

$$p_{\text{HDA-LDA}}(T) = (190 - T * 0.26) \text{ MPa}. \quad (1)$$

That is, HDA and LDA are expected to have equal chemical potential, e.g., at 100 K and 164 MPa. Detailed studies of isothermal compression and decompression of LDA and HDA found a hysteresis for the transition that becomes smaller at higher temperatures, again pointing towards a first-order-like transition and yielding an estimated equilibrium pressure consistent with Eq. (1).³² Further evidence in favour of a first-order-like nature of the transition was found in neutron scattering experiments, both at 1 bar⁴⁶ and at high pressure,⁴⁷ and in calorimetric studies at ambient pressure.^{33,42,43,48–50} Some authors even reported the observation of macroscopic phase separation.^{33,47,51,52} Additional support was provided through Raman spectroscopy,⁵³ ultrasonic experiments,^{54–56} and further scattering experiments⁵⁷ as well as from studies on water in protein crystals⁵⁸ and aqueous solutions.^{59–65} Also measurements of the thermal conductivity show a sharp change when HDA transforms to LDA.⁶⁶ The authors of Ref. 66, however, express their doubts regarding a separation of HDA and LDA.

Arguments in favour of a continuous HDA \rightarrow LDA transition were also inferred from neutron and X-ray scattering experiments, where the intermediate states could not be fitted as linear combinations of LDA and HDA.^{67–69} This apparent contradiction might be resolved by the very recent study of Perakis *et al.*³¹ In monitoring the HDA \rightarrow LDA transition of sufficiently relaxed HDA samples, Perakis *et al.* showed that it is indeed possible to separate the intermediate states in a LDA and a HDA contribution.³¹ Unrelaxed samples, however, do not display this behaviour but show a more complex transition,³¹ consistent with the assessment of Ref. 56 and the abovementioned studies.^{67–69} In summary, most studies seem to favour a first-order-like transition occurring between HDA and LDA.

D. The relation between VHDA and LDA

The VHDA \rightarrow LDA transition was studied almost exclusively by isobaric heating at 1 bar. Neutron scattering indicates a relaxation of VHDA preceding the transformation to LDA.⁷⁰ This relaxation produces states similar to HDA, leading to the conclusion that the states observed in the HDA \rightarrow LDA transition are a subset of the states found in the VHDA \rightarrow LDA transition and that the final stage of the transformation bears all signs of a first-order-like transition.⁷¹ Similar results were obtained from ²H-NMR measurements.⁷² During the VHDA \rightarrow LDA transition at 1 bar, VHDA was found to relax continuously toward HDA which in turn transforms to LDA.⁷² In addition, calorimetry scans of VHDA at 1 bar reveal enthalpy relaxation (presumably toward HDA) preceding the sudden release of heat indicating the polyamorphic transition to LDA.⁷³ Finally, studies of the isothermal decompression

of VHDA at $T \geq 125$ K showed that VHDA continuously evolves into HDA which in turn transforms discontinuously to LDA if the temperature is sufficiently high.^{41,74} In summary, all published studies are consistent with a first-order-like transition from VHDA to LDA. Yet, a relaxation from VHDA to HDA precedes the transformation to LDA in all cases. Hence, the relation between VHDA and HDA is relevant also for the VHDA \rightarrow LDA transition and cannot be completely excluded here.

E. Aim of this work

The available studies on the polyamorphism of water typically obtain LDA by heating uHDA at ambient pressure or sometimes by decompressing HDA at $T \approx 130$ – 140 K close to ambient pressure. What is missing in the literature is an analysis of the nature of the isobaric transitions of amorphous ices at elevated pressure and starting from differently prepared samples.

In other studies, we have investigated the (isobaric) temperature-induced amorphisation of hexagonal ice,⁷⁵ the (isobaric) temperature-induced relaxations,⁷⁶ and transformations⁴⁴ of eHDA and VHDA. Here, we study the isobaric transitions of several amorphous ices to LDA at 4 MPa. This expands the frontiers of knowledge gained from studies at ambient pressure.^{31,33,42} Most notably, raising the pressure increases the temperature window in which the high-density amorphous forms can be studied prior to the transformation to LDA.³² This allows us to study the nature of relaxations up to higher temperatures, enabling us to actually demonstrate that metastable equilibrium can be reached on the experimental time scale. That is, even below the border to the no-man's land, thermodynamic histories become irrelevant. In order to achieve just this, it is our concept to use several different initial amorphous states and to test whether or not there is path independence for the states reached at 4 MPa. We are especially interested how the path picked influences the amount of relaxation occurring prior to the transformation to LDA. To this end, we compare well established initial states (uHDA, eHDA, and VHDA) and amorphous states specifically selected for the present study (uHDA and VHDA relaxed at 0.1 GPa; details follow below). The isobaric transitions themselves are monitored by *in situ* volumetry, and the samples are

further characterized *ex situ* using powder X-ray diffraction (XRD).

II. EXPERIMENTAL DETAILS

In order to produce the different samples, 500 μl of pure water were pipetted into a preformed indium container ($m \approx 320$ mg) at 77 K. Indium serves as a low-temperature lubricant, a technique pioneered by Mishima *et al.*³⁶ The samples were then put in a high-pressure cell of 8 mm bore diameter, and the cell was subsequently placed in a material testing machine (Zwick model BZ100/TL3S; for details on our apparatus, see Ref. 77). The pressure was raised to 1.0 GPa at 77 K to push the air out of the sample, reduced to 0.02 GPa, and subsequently raised again to 1.5–1.7 GPa with 0.14 GPa min^{-1} . During the last step, the ice sample transforms to uHDA via PIA. After reducing the pressure to 1.1 GPa (uHDA at 1.1 GPa and 77 K), the steps listed in Table I were performed to produce a range of samples. The abbreviations listed in Table I are used in the following to refer precisely to the respective route of production.

The pressure was then reduced at 77 K to 4 MPa, and, finally, as the key step analysed in this work, the samples were heated isobarically with 3 K min^{-1} to temperatures up to 155 K. This transforms the samples to LDA in all cases, which were then quenched with liquid N_2 and recovered to ambient pressure. The p - T steps performed for the different samples are visualised in Fig. 1. All transformations were monitored using *in situ* dilatometry by recording the piston displacement. The piston displacement curves were transformed to change of volume curves assuming constant cell diameter and corrected for the apparatus behaviour by subtracting a blind experiment. For the blind experiment, we perform the same steps as for the real experiment, leaving only the water out. Thus, we are able to record the behaviour of the apparatus and indium along the studied paths as a reference (cf. Ref. 78).

For the purpose of recording X-ray diffractograms, the samples were first divided into two or three pieces, and each piece was powdered and measured separately. Hence, two or three diffractograms were recorded per sample. Division and powdering were performed under liquid N_2 . The powder was cold-loaded onto a precooled (≈ 80 K) nickel-plated copper

TABLE I. Temperature and pressure program for sample production starting from uHDA at 1.1 GPa and 77 K. Here q and π denote the heating and decompression rate, respectively. The steps were performed left to right and thereafter the temperature was brought to 77 K. In all cases, the cooling rate was not controlled. Ultimately, all samples were quenched with liquid N_2 and decompressed to 4 MPa. Note that uHDA(0.1) crystallizes partly during the low p annealing step.

Sample	High p annealing			Decompression			Low p annealing		
	p (GPa)	T_{max} (K)	q (K min^{-1})	T (K)	p_{min} (GPa)	π (GPa min^{-1})	p (GPa)	T_{max} (K)	q (K min^{-1})
uHDA
uHDA(0.1)	77	0.1	0.14	0.1	140	3
VHDA	1.1	160	3
VHDA(0.1)	1.1	160	3	77	0.1	0.14	0.1	140	3
eHDA(0.1)	1.1	160	3	140	0.1	0.02
eHDA(0.2)	1.1	160	3	140	0.2	0.02

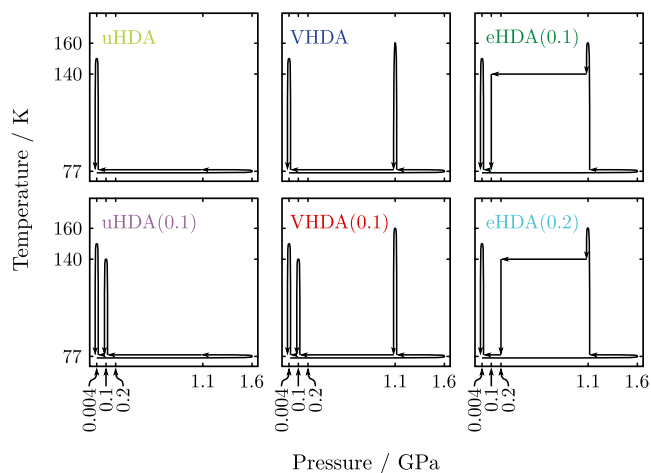


FIG. 1. p - T diagrams showing the paths utilised for the six types of amorphous ice samples studied here. Each path starts with hexagonal ice which is amorphised during the initial compression at 77 K and each path ends with the isobaric heating at 4 MPa, where the *in situ* volume changes are reported in Fig. 2. After this final heating step, the samples are quenched to 77 K, decompressed to ambient pressure, and stored in liquid N_2 .

sample holder in flat geometry. The low-temperature chamber by Anton-Paar (TTK 450) holding the sample holder is then closed and pumped to approximately 10^{-2} mbar. We used a Siemens D 5000 diffractometer equipped with a $Cu-K\alpha$ X-ray source ($\lambda = 1.541 \text{ \AA}$) to record the diffractograms at $\approx 80 \text{ K}$ from $2\theta = 10^\circ$ ($K = 0.71 \text{ \AA}^{-1}$) to $2\theta = 54^\circ$ ($K = 3.70 \text{ \AA}^{-1}$) using a step width of 0.02° and an acquisition time of 1 s per step.

For comparison, also an ice II sample was produced following the protocol given in Ref. 79. 500 μl of pure water were frozen to hexagonal ice in the same manner as explained above, compressed to 0.4 GPa at 198 K with a rate of $0.001 \text{ GPa min}^{-1}$, and quenched with liquid N_2 upon reaching 0.4 GPa. Thereafter the sample was decompressed at 77 K to 4 MPa with a rate of $0.002 \text{ GPa min}^{-1}$, where it was heated isobarically with 3 K min^{-1} to record its expansivity.

III. IN SITU VOLUMETRY

The *in situ* volumetric results for the transitions to LDA at 4 MPa are shown in Fig. 2. The curves differ for each starting material. They differ both quantitatively and qualitatively. The two quantitative measures assessed here are step-height, i.e., the volume-difference with respect to LDA, and the onset temperature of the transformation. The corresponding results are summarised in Table II.

The largest step-height is observed for VHDA. It is followed by eHDA(0.2), uHDA, eHDA(0.1), VHDA(0.1), and finally uHDA(0.1). The sequence until eHDA(0.1) is in accord with the known densities at 1 bar for those samples.³⁵ VHDA being the most dense form shows the largest step and it is followed by eHDA(0.2), uHDA, and eHDA(0.1). Next in line is VHDA(0.1) for which almost the same step-height as for eHDA(0.1) is found at 4 MPa, indicating that those two forms are very similar. Finally, we find that uHDA(0.1) shows the lowest step-height. This result, however, is flawed since the sample partially crystallizes during annealing at 0.1 GPa as apparent from XRD measurements after transition to LDA (not shown). That uHDA gradually crystallizes when heated at

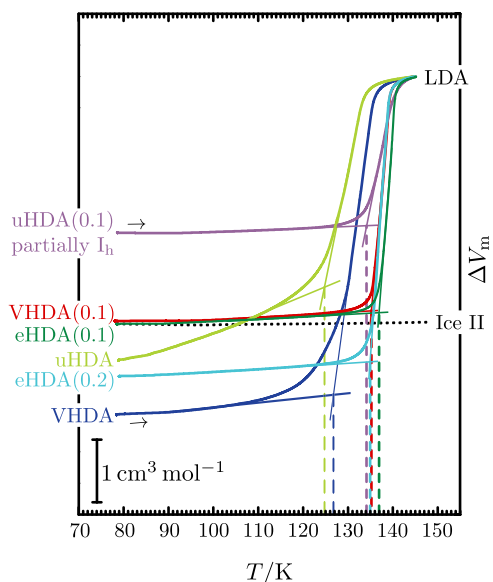


FIG. 2. Change of molar volume during isobaric transformation of several amorphous ices to LDA at 4 MPa. The coloured dashed lines mark the onset temperatures, and the black dotted line shows the behaviour of ice II.

similar pressures is well known,^{80–83} and it was reported that roughly 40% of an uHDA sample crystallized after heating to 135 K at 0.1 GPa.⁸⁰ Assuming that also the uHDA(0.1) sample consists of 40% hexagonal ice, the real difference in molar volume between uHDA(0.1) and LDA can be estimated. This estimation yields $\approx 4.2 \text{ cm}^3 \text{ mol}^{-1}$ for the volume difference between uHDA(0.1) and LDA, a similar value as found for eHDA(0.1) and VHDA(0.1) indicating that the amorphous part of uHDA(0.1) is also similar to eHDA(0.1) (cf. Table II).

Now we want to take a close look on the implications of the ordering described above. We first look at the sequence VHDA, eHDA(0.2), uHDA, and eHDA(0.1), which is interesting in two ways. First, as visible from Table II, the step-height of eHDA(0.2) is halfway between the ones of VHDA and eHDA(0.1). Since both eHDA(0.1) and eHDA(0.2) are produced via the decompression of VHDA at 140 K (cf. Table I and Fig. 1), this means that about half of the volume change upon decompressing VHDA from 1.1 GPa to 0.1 GPa occurs between 0.2 and 0.1 GPa. A similar finding was reported for the shift of the calorimetric transition temperatures to LDA at 1 bar.³³ According to Fig. 3(b) of Ref. 33, the peak transition temperatures are 126 K for VHDA, 131 K for eHDA(0.2), and

TABLE II. Total volume changes and onset temperatures of the transition to LDA at 4 MPa. The temperatures were determined from Fig. 2 using the tangent method. For uHDA(0.1), the ΔV_m value is flawed due to the presence of ice I_h . An estimate for the correct value assuming 40% crystallization⁸⁰ is given in parentheses.

Sample	ΔV_m ($\text{cm}^3 \text{ mol}^{-1}$)	T (K)
VHDA	5.4	127
eHDA(0.2)	4.8	135
uHDA	4.5	125
eHDA(0.1)	4.0	137
VHDA(0.1)	3.9	135
uHDA(0.1)	2.5 (≈ 4.2)	134

134 K for eHDA(0.07) (in Ref. 33, the VHDA decomposition at 140 K was quenched at 0.07 GPa). Again, about half of the change occurs between 0.2 and 0.07 GPa. Second, it is interesting to note that eHDA(0.2) is denser than uHDA. When considering that uHDA expands when heated below 0.35 GPa^{84,85} and that it only densifies when heated at higher pressures,⁸⁵ it is implied that eHDA(0.2) cannot be reached by simply heating uHDA at 0.2 GPa. Heating uHDA at 0.2 GPa would yield less dense samples than uHDA. eHDA(0.2), however, is denser than uHDA and thus the path how one reaches 0.2 GPa and 140 K starting from uHDA at 1.1 GPa and 77 K is relevant. This indicates that at least one of the two forms has not reached metastable equilibrium at 140 K and 0.2 GPa. This implication of the volume changes during the transformation to LDA at 4 MPa seems inconsistent with Winkel *et al.*'s finding that eHDA(0.2) and uHDA heated at 0.2 GPa to 140 K are practically the same form and that metastable equilibrium is reached at this pressure and temperature conditions.³³ To reconcile these opposing findings, the following two things have to be taken into account. First, studies of the glass-to-liquid transition of different HDAs at 0.2 GPa yield glass-to-liquid transition temperatures between ≈ 140 and ≈ 150 K.^{42,80,86,87} Second, Winkel *et al.*'s study³³ is based on calorimetry and XRD, not volumetry. Considering these two points, we believe that details of the experiment and analysis procedure can push the result to one or the other side. Therefore, eHDA(0.2) might be close to metastable equilibrium at 140 K and 0.2 GPa, but this state cannot be reached by simply heating uHDA at 0.2 GPa to this temperature.

The last part of the sequence is eHDA(0.1), VHDA(0.1), and uHDA(0.1) and all of them show a very similar density, indicating that those three different paths yield very similar samples (mind the correction of the uHDA(0.1) value; cf. Table II). It has to be recognised, however, that during heating of uHDA at 0.1 GPa two changes occur in parallel. The amorphous matrix relaxes and crystallizes simultaneously. Despite the fact that substantial parts of the sample crystallize, the amorphous matrix of uHDA(0.1) relaxes toward eHDA(0.1) at 140 K, indicating path independence. When comparing VHDA(0.1) and eHDA(0.1), this apparent path independence becomes even clearer. Figure 3 compares the volume change along both the eHDA(0.1) and VHDA(0.1) paths. Both paths end up very close to each other at 0.1 GPa and 140 K but follow an entirely different route. Therefore, metastable equilibrium is indeed reached at 0.1 GPa and 140 K, i.e., the relaxation time is shorter than the experimental time scale and faster than the crystallization time scale. This finding is also consistent with the reported temperatures for the glass-to-liquid transition of different HDAs at 0.1 GPa, which were reported to lie around or below 140 K.^{42,80,86,87}

The second quantitative measure assessed here is the onset temperature of the major step indicating the transition to LDA. This temperature is also dependent on the starting amorphous form (see Table II and Fig. 2). It is obvious that the samples previously relaxed at 0.1 or 0.2 GPa [uHDA(0.1), VHDA(0.1), eHDA(0.1), eHDA(0.2)] have a very similar onset, whereas uHDA and VHDA show an onset temperature that is lower by ≈ 10 K. This is a manifestation of the different initial degree of relaxation of the samples. At 4 MPa, uHDA and VHDA

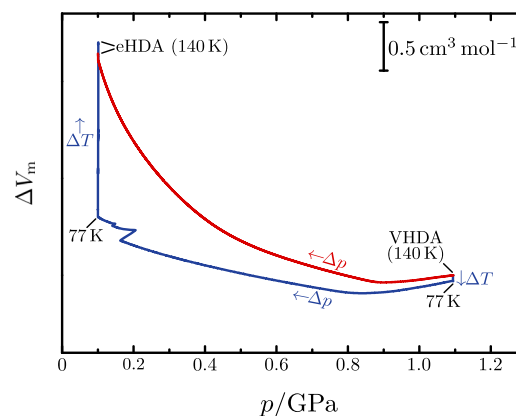


FIG. 3. Comparison of the *in situ* volume curves of the eHDA(0.1) production path (red) and the VHDA(0.1) production path (blue). Both paths start with VHDA at 140 K and 1.1 GPa and end at 140 K and 0.1 GPa.

are not well relaxed, whereas the other forms are. The similar onset of uHDA(0.1) and the other low pressure relaxed forms further indicates that the amorphous part of this sample is well relaxed and that the ice I_h fraction is unlikely to influence the polyamorphic transition to LDA.

Regarding the qualitative behaviour of the curves shown in Fig. 2, one can clearly see that all low-pressure relaxed samples show very flat curves prior to the major step. This behaviour is almost comparable to the heating curve of ice II (dotted line in Fig. 2) signifying that those samples do not significantly relax prior to the transition to LDA. The curves of the unrelaxed sample (uHDA) and the sample relaxed at 1.1 GPa (VHDA) on the contrary show a pronounced non-linear behaviour prior to the major step. This indicates that those two forms relax significantly during heating at 4 MPa, indicating a non-equilibrium structure. The step itself is very sharp for the low-pressure annealed HDA forms, whereas it is much broader for VHDA and uHDA. This suggests an interpretation of the step as a first-order-like transition from uHDA(0.1), VHDA(0.1), eHDA(0.1), and eHDA(0.2) to LDA. Nevertheless, we also interpret the transitions from VHDA and uHDA to LDA as first-order-like transitions. In the latter cases, however, a non-linear relaxation is superimposed. For eHDA(0.2), also a relaxation is expected to occur since its density is quite different from eHDA(0.1). The curve is, however, very flat prior to the transition meaning that for eHDA(0.2), relaxation and transformation take place in a very similar temperature interval and the two processes cannot be disentangled with our methods. Furthermore, it has to be noted that the eHDA(0.1) and VHDA(0.1) curves almost lie on top of each other, again supporting the path independence in this case (cf. Fig. 2).

IV. EX SITU X-RAY DIFFRACTION

In order to corroborate the above analysis, we studied three transitions in more detail. Those transitions are uHDA \rightarrow LDA, VHDA \rightarrow LDA, and eHDA(0.1) \rightarrow LDA (cf. Fig. 2), all of which were quenched at several intermediate temperatures. The corresponding samples were then recovered to ambient pressure and characterized by XRD. In the

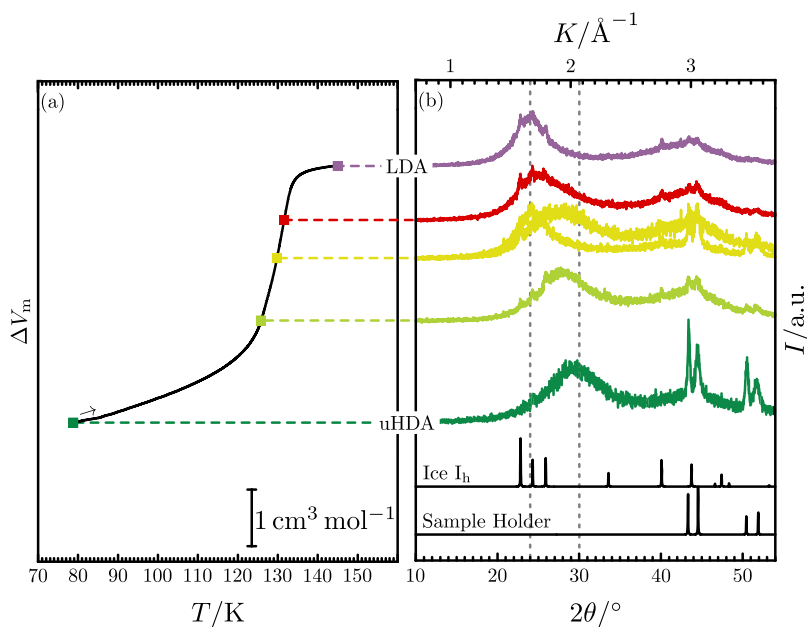


FIG. 4. XRD-analysis of intermediate states of the uHDA \rightarrow LDA transition at 4 MPa. (a) shows the volume change (cf. Fig. 2) and the points mark temperatures where samples were quenched and recovered to ambient pressure. The corresponding diffractograms after quench-recovery are shown in (b). Two diffractograms with the same colour stem from the same sample. The dotted grey line at 24.0° (1.69 \AA^{-1}) marks the position of the first diffraction maximum for LDA according to Refs. 48 and 41. The dotted grey line at 30.0° (2.11 \AA^{-1}) aids seeing shifts in the first diffraction maximum of uHDA. The black diffractograms at the bottom are calculated diffractograms of hexagonal ice and the nickel-plated copper sample holder using PowderCell (version 2.4, BAM, Bundesanstalt für Materialforschung und -prüfung, Berlin, Germany). The relevant structural data were taken from Refs. 90 and 91, respectively.

following, we discuss the position of the first diffraction maximum ($2\theta_{\text{max}}$) in the course of the transition.

Figure 4 shows the quench temperatures and corresponding XRD measurements for the uHDA \rightarrow LDA transition. At $\approx 126 \text{ K}$ (light green), the first diffraction maximum slightly shifts to lower angles. However, no LDA is present to this point. This means that the volume change up to this temperature is influenced solely by relaxation. At $\approx 130 \text{ K}$ (yellow) also LDA is found in the XRD measurements. The measurement of one part of the sample shows the characteristics of LDA with the first diffraction maximum around 24° , whereas the measurement of another part of the same sample shows a very broad maximum. This broad maximum indicates the coexistence of relaxed uHDA and LDA. Although no clear separation of the two corresponding maxima was found, it was still possible to fit the broad maximum with two Lorentzians at LDA and HDA positions as shown in Fig. 5. Since the LDA contribution to this broad maximum is rather small, this part of the sample consists of a small amount of LDA and a large amount of relaxed uHDA. At $\approx 132 \text{ K}$ (red), the sample consists mostly of LDA, with a slight shoulder indicating also some relaxed uHDA to be present. At $\approx 145 \text{ K}$ finally (purple), the sample consists of pure LDA. These results again show that in the first stage of heating the uHDA matrix relaxes (marked by a shift of the first diffraction maximum), which is followed by a first-order-like polyamorphic transition to LDA (marked by the coexistence of LDA and relaxed uHDA).

Figure 6 shows the quench temperatures and corresponding XRD measurements for the VHDA \rightarrow LDA transition. The XRD characteristics barely change upon heating to $\approx 114 \text{ K}$ (light blue and dark blue). At $\approx 130 \text{ K}$ (dark green), the measurements of the two parts of the sample look completely different. One part shows a clearly shifted maximum compared to the initial VHDA, and the other part shows almost pure LDA. This is therefore a clear case of macroscopic phase separation, strongly pointing towards a first-order-like transition. A very similar result is obtained at $\approx 132 \text{ K}$ (light green). At $\approx 134 \text{ K}$

(yellow), a broad maximum was found that again could be fitted with two Lorentzians (see Fig. 5). At temperatures above $\approx 145 \text{ K}$ finally (red and purple), the sample consists of pure

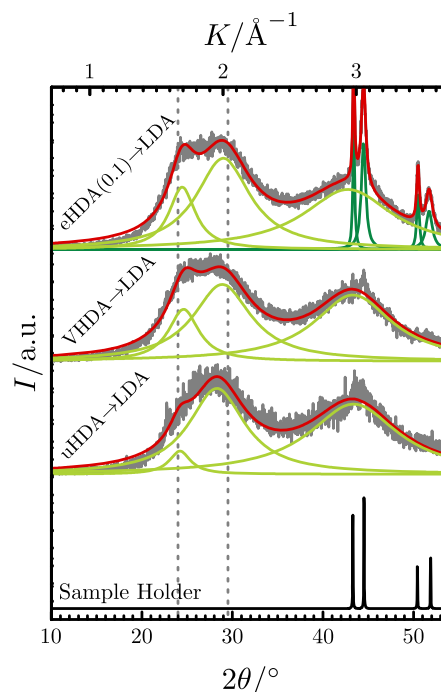


FIG. 5. Examples for fits of XRD measurements of intermediate states of the eHDA(0.1) \rightarrow LDA, VHDA \rightarrow LDA, and uHDA \rightarrow LDA transitions. The transition was quenched at $\approx 139 \text{ K}$ [eHDA(0.1)], $\approx 134 \text{ K}$ (VHDA), and $\approx 130 \text{ K}$ (uHDA). The fit (red) is composed of Lorentzians for the amorphous sample (light green) and the sample holder (dark green). The dotted grey line at 24.0° (1.69 \AA^{-1}) marks the position of the first diffraction maximum for LDA according to Refs. 48 and 41. The dotted grey line at 29.5° (2.08 \AA^{-1}) marks the approximate position of the first diffraction maximum for uHDA and eHDA(0.1). The black diffractogram at the bottom is the calculated diffractogram of the nickel-plated copper sample holder using PowderCell (version 2.4, BAM, Bundesanstalt für Materialforschung und -prüfung, Berlin, Germany). The relevant structural data were taken from Ref. 91.

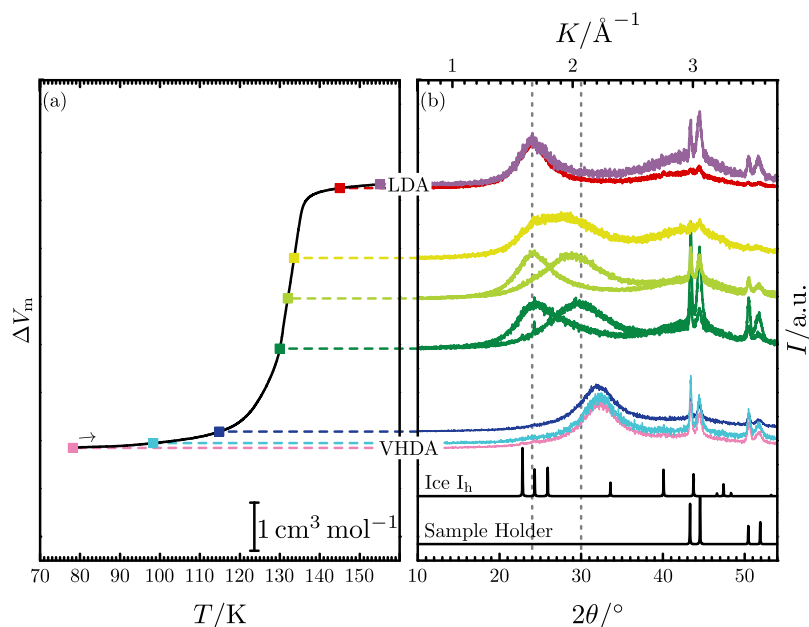


FIG. 6. Analogous to Fig. 4 for the VHDA \rightarrow LDA transition at 4 MPa.

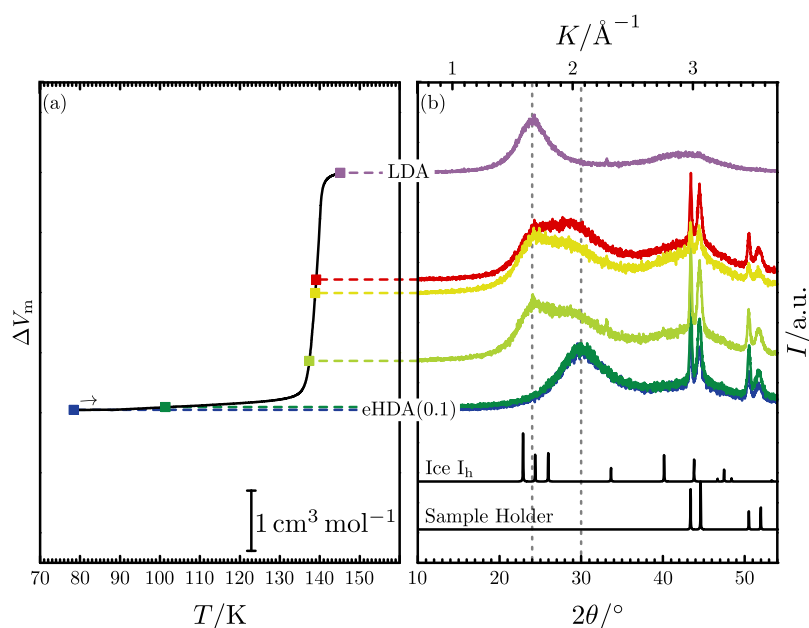


FIG. 7. Analogous to Fig. 4 for the eHDA(0.1) \rightarrow LDA transition at 4 MPa.

LDA. The results for VHDA also confirm the above analysis. When VHDA is heated at 4 MPa, it first undergoes a relaxation (marked by a shift of the first diffraction maximum), which is followed by a first-order-like polyamorphic transition to LDA (marked by the coexistence of LDA and relaxed VHDA).

Figure 7 finally shows the quench temperatures and corresponding XRD measurements for the eHDA(0.1) \rightarrow LDA transition. Here no shift in the first diffraction maximum was found after heating to ≈ 101 K (dark green). When quenched in the middle of the step ≈ 137 – 139 K (light green, yellow, and red), broad first diffraction maxima were found. They again indicate the coexistence of slightly relaxed eHDA(0.1) and LDA according to a fit with two Lorentzians (cf. Fig. 5). At ≈ 145 K finally (purple), the sample consists of pure LDA. Also here the above analysis is confirmed. eHDA(0.1) barely relaxes before it transforms to LDA, but

again the transformation to LDA itself seems to be first-order-like [marked by the coexistence of LDA and relaxed eHDA(0.1)].

V. COMBINING VOLUMETRY AND XRD

Figure 8 summarizes the results of the detailed XRD analysis of the polyamorphic transitions. All positions of the first diffraction maxima as a function of quench temperature are shown. In principle, three regimes can be separated: the VHDA regime ($2\theta > 32^\circ$), the HDA regime ($28^\circ \leq 2\theta \leq 32^\circ$) and the LDA regime ($2\theta \approx 24^\circ$). Based on the jump-like change from the high-density maxima at lower temperatures to LDA at higher temperatures (indicated by the dashed lines), all three transitions seem to be first-order-like transitions. For eHDA(0.1), barely any relaxation is found before the step, as expected from the flat volume curves in the lower temperature

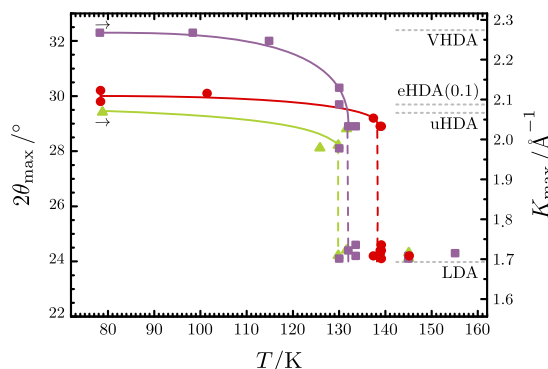


FIG. 8. Positions of the first diffraction maximum for states along the uHDA \rightarrow LDA (triangles), VHDA \rightarrow LDA (squares), and eHDA(0.1) \rightarrow LDA (circles) transitions as a function of quench temperature. The solid coloured lines are guides to the eye and the corresponding dashed lines mark the jumps of the first diffraction maxima. The grey dotted lines mark the positions of the first diffraction maximum for uHDA, VHDA, eHDA(0.1), and LDA.

part. VHDA displays a continuous change of the maximum from $2\theta > 32^\circ$ to $2\theta \approx 28^\circ$ before the transition to LDA. This shift is a relaxation of the amorphous matrix towards HDA according to our XRD results, a relaxation also reflected in the non-linear low temperature behaviour of VHDA in volumetry. For uHDA, shifts to smaller angles preceding the transition to LDA were found in XRD. Those changes, however, are small compared to the VHDA case. This clearly contrasts with the behaviour of uHDA in volumetry, where a considerable amount of volume relaxation was found. Therefore, it seems that the low-temperature volume change in uHDA is caused by a more complex type of relaxation. One additional process we know of is the growth of the crystalline residues present in uHDA^{82,83} as is visible by the appearance of small hexagonal ice reflexes in the XRD measurements of the uHDA \rightarrow LDA transition (cf. Fig. 3). This small amount of crystallization, however, cannot be the reason for the different behaviour of uHDA and VHDA in the low temperature part of the heating.

VI. SUMMARY AND CONCLUSION

In our study of the isobaric heating of several high-density amorphous ices at 4 MPa, we find that of all the samples studied VHDA and uHDA relax considerably prior to the transformation to LDA. The volume changes of the two forms show clear non-linear behaviour prior to the polymorphic transition to LDA. In XRD measurements of intermediate states of the VHDA \rightarrow LDA transition, relaxation behaviour of VHDA was also found. Its first diffraction maximum shifts to values typical for HDA prior to the transformation. For the uHDA \rightarrow LDA transition, however, a relaxation was not so clearly visible in XRD measurements of the intermediate states (cf. Fig. 7), but clearly evident in the volumetry curves (cf. Fig. 2).

The other forms studied behave almost like crystals in the lower temperature region in terms of their thermal expansion, indicating that these forms are well relaxed. Although showing a very flat curve prior to the transition, eHDA(0.2) is not as well relaxed as uHDA(0.1), VHDA(0.1), or eHDA(0.1). This indicates that eHDA(0.2) relaxes right before the

transition to LDA, making a clear separation of the time scales for relaxation and transition difficult.

The transition to LDA at higher temperatures is seen to obey criteria for a first-order-like transition in all cases. We found very sharp transitions for eHDA(0.1), eHDA(0.2), VHDA(0.1), and uHDA(0.1). Furthermore, the detailed studies of uHDA, VHDA, and eHDA(0.1) indicate coexistence with LDA in the XRD in the middle of the transition (cf. Fig. 5). In the case of VHDA, even macroscopic phase separation was observed (cf. Fig. 6). The coexistences found for uHDA and VHDA further show that the less sharp transition steps in those cases can be explained as a combined effect of relaxation and transformation. In summary, all samples studied share the feature of a first-order-like transition to LDA. For uHDA and VHDA, the transition is, however, partially obscured by relaxation. This is similar to findings at ambient pressure for uHDA⁴⁹ and VHDA.^{70–73} The strong influence of sample preparation on the transition is further in accord with very recent numerical studies utilising the potential energy landscape formalism.^{88,89} These studies have shown that (although the LDA \rightarrow HDA transformation behaves as a first-order like transition⁸⁸) the choice of the initial LDA strongly influences the nature of the transformations.⁸⁹ In any case, our findings are in agreement with the view that HDA and LDA are two distinct polyamorphs. It has to be emphasised that the sharpest transformation is found for eHDA(0.1), again showing that it is a very well relaxed HDA at lower pressures. Relaxing uHDA at low pressures should be avoided if the study of well-relaxed HDA is desired, since considerable amounts of the sample crystallize during this relaxation.

Finally we note that it seems that the metastable equilibrium is reached at 0.1 GPa and 140 K since the eHDA(0.1) and VHDA(0.1) samples behave very similarly. This is most clearly visible in Fig. 3, where the two different paths end up at the same molar volume. The low-pressure annealing step for uHDA on the contrary leads to significant crystallization of the uHDA(0.1) sample although the remainder of the amorphous sample appears to be well relaxed, consistent with the metastable equilibrium at 0.1 GPa and 140 K. This finding is in agreement with several studies concerned with the glass transition of HDA.^{42,80,86,87} We also conclude based on the density of eHDA(0.2) that the metastable equilibrium appears not to be reached at 0.2 GPa and 140 K. However, we also find that about half of the volume change from VHDA to eHDA(0.1) happens between 0.2 and 0.1 GPa, indicating that the sample is at the verge of the metastable equilibrium at 140 K and 0.2 GPa.

ACKNOWLEDGMENTS

We thank Katrin Amann-Winkel for helpful discussions. P.H.H. and T.L. gratefully acknowledge funding by the Austrian Science Fund FWF (Erwin Schrödinger Fellowship No. J3811 N34 and bilateral Project No. I1392, respectively).

¹L. G. M. Pettersson, R. H. Henchman, and A. Nilsson, “Water—The most anomalous liquid,” *Chem. Rev.* **116**, 7459 (2016).

²C. A. Angell, *Annu. Rev. Phys. Chem.* **55**, 559–583 (2004).

³P. G. Debenedetti, *J. Phys.: Condens. Matter* **15**(45), R1669–R1726 (2003).

- ⁴P. Gallo, K. Amann-Winkel, C. A. Angell, M. A. Anisimov, F. Caupin, C. Chakravarty, E. Lascaris, T. Loerting, A. Z. Panagiotopoulos, J. Russo *et al.*, *Chem. Rev.* **116**(13), 7463–7500 (2016).
- ⁵P. H. Handle, T. Loerting, and F. Sciortino, *Proc. Natl. Acad. Sci. U. S. A.* **114**(51), 13336–13344 (2017).
- ⁶O. Mishima and H. Stanley, *Nature* **396**(6709), 329–335 (1998).
- ⁷F. H. Stillinger and A. Rahman, *J. Chem. Phys.* **60**(4), 1545–1557 (1974).
- ⁸J. C. Palmer, F. Martelli, Y. Liu, R. Car, A. Z. Panagiotopoulos, and P. G. Debenedetti, *Nature* **510**(7505), 385–388 (2014).
- ⁹P. H. Poole, F. Sciortino, U. Essmann, and H. Stanley, *Nature* **360**(6402), 324–328 (1992).
- ¹⁰F. Smallenburg and F. Sciortino, *Phys. Rev. Lett.* **115**(1), 015701 (2015).
- ¹¹J. L. Abascal and C. Vega, *J. Chem. Phys.* **123**(23), 234505 (2005).
- ¹²C. Vega and J. L. Abascal, *Phys. Chem. Chem. Phys.* **13**(44), 19663–19688 (2011).
- ¹³J. L. Abascal and C. Vega, *J. Chem. Phys.* **133**(23), 234502 (2010).
- ¹⁴J. W. Biddle, R. S. Singh, E. M. Sparano, F. Ricci, M. A. González, C. Valeriani, J. L. Abascal, P. G. Debenedetti, M. A. Anisimov, and F. Caupin, *J. Chem. Phys.* **146**(3), 034502 (2017).
- ¹⁵S. Overduin and G. Patey, *J. Chem. Phys.* **138**(18), 184502 (2013).
- ¹⁶S. Overduin and G. Patey, *J. Chem. Phys.* **143**(9), 094504 (2015).
- ¹⁷R. S. Singh, J. W. Biddle, P. G. Debenedetti, and M. A. Anisimov, *J. Chem. Phys.* **144**(14), 144504 (2016).
- ¹⁸T. Sumi and H. Sekino, *RSC Adv.* **3**(31), 12743–12750 (2013).
- ¹⁹T. Yagasaki, M. Matsumoto, and H. Tanaka, *Phys. Rev. E* **89**(2), 020301 (2014).
- ²⁰O. Mishima, *J. Chem. Phys.* **133**(14), 144503 (2010).
- ²¹O. Mishima and H. Stanley, *Nature* **392**(6672), 164–168 (1998).
- ²²O. Mishima, *Phys. Rev. Lett.* **85**(2), 334–336 (2000).
- ²³H. Laksmono, T. A. McQueen, J. A. Sellberg, N. D. Loh, C. Huang, D. Schlessinger, R. G. Sierra, C. Y. Hampton, D. Nordlund, M. Beye *et al.*, *J. Phys. Chem. Lett.* **6**(14), 2826–2832 (2015).
- ²⁴P. Brüggeller and E. Mayer, *Nature* **288**(5791), 569–571 (1980).
- ²⁵E. Mayer, *J. Appl. Phys.* **58**(2), 663–667 (1985).
- ²⁶I. Kohl, L. Bachmann, A. Hallbrucker, E. Mayer, and T. Loerting, *Phys. Chem. Chem. Phys.* **7**(17), 3210–3220 (2005).
- ²⁷O. Mishima and Y. Suzuki, *J. Chem. Phys.* **115**(9), 4199–4202 (2001).
- ²⁸P. H. Poole, T. Grande, F. Sciortino, H. E. Stanley, and C. A. Angell, *Comput. Mater. Sci.* **4**(4), 373–382 (1995).
- ²⁹C. R. Hill, C. Mitterdorfer, T. G. Youngs, D. T. Bowron, H. J. Fraser, and T. Loerting, *Phys. Rev. Lett.* **116**(21), 215501 (2016).
- ³⁰K. Amann-Winkel, C. Gainaru, P. H. Handle, M. Seidl, H. Nelson, R. Böhmer, and T. Loerting, *Proc. Natl. Acad. Sci. U. S. A.* **110**(44), 17720–17725 (2013).
- ³¹F. Perakis *et al.*, *Proc. Natl. Acad. Sci. U. S. A.* **114**(31), 8193–8198 (2017).
- ³²O. Mishima, *J. Chem. Phys.* **100**(8), 5910–5912 (1994).
- ³³K. Winkel, E. Mayer, and T. Loerting, *J. Phys. Chem. B* **115**(48), 14141–14148 (2011).
- ³⁴S. Lemke, P. H. Handle, L. Plaga, J. N. Stern, M. Seidl, V. Fuentes-Landete, K. Amann-Winkel, K. Köster, C. Gainaru, T. Loerting, and R. Böhmer, *J. Chem. Phys.* **147**(3), 034506 (2017).
- ³⁵T. Loerting, M. Bauer, I. Kohl, K. Watschinger, K. Winkel, and E. Mayer, *J. Phys. Chem. B* **115**(48), 14167–14175 (2011).
- ³⁶O. Mishima, L. D. Calvert, and E. Whalley, *Nature* **310**(5976), 393–395 (1984).
- ³⁷O. Mishima, L. D. Calvert, and E. Whalley, *Nature* **314**(6006), 76–78 (1985).
- ³⁸T. Loerting, C. Salzmänn, I. Kohl, E. Mayer, and A. Hallbrucker, *Phys. Chem. Chem. Phys.* **3**(24), 5355–5357 (2001).
- ³⁹C. G. Salzmänn, T. Loerting, S. Klotz, P. W. Mirwald, A. Hallbrucker, and E. Mayer, *Phys. Chem. Chem. Phys.* **8**(3), 386–397 (2006).
- ⁴⁰R. J. Nemes, J. S. Loveday, T. Strässle, C. L. Bull, M. Guthrie, G. Hamel, and S. Klotz, *Nat. Phys.* **2**(6), 414–418 (2006).
- ⁴¹K. Winkel, M. S. Elsaesser, E. Mayer, and T. Loerting, *J. Chem. Phys.* **128**(4), 044510 (2008).
- ⁴²P. H. Handle, M. Seidl, and T. Loerting, *Phys. Rev. Lett.* **108**(22), 225901 (2012).
- ⁴³O. Mishima, *Nature* **384**(6609), 546–549 (1996).
- ⁴⁴P. H. Handle and T. Loerting, *J. Chem. Phys.* **148**(12), 124509 (2018).
- ⁴⁵E. Whalley, D. D. Klug, and Y. P. Handa, *Nature* **342**(6251), 782–783 (1989).
- ⁴⁶M. M. Koza, H. Schober, H. E. Fischer, T. Hansen, and F. Fujara, *J. Phys.: Condens. Matter* **15**(3), 321–332 (2003).
- ⁴⁷S. Klotz, T. Strässle, R. J. Nemes, J. S. Loveday, G. Hamel, G. Rouse, B. Canny, J. C. Chervin, and A. M. Saitta, *Phys. Rev. Lett.* **94**(2), 025506 (2005).
- ⁴⁸A. Bizid, L. Bosio, A. Defrain, and M. Oumezzine, *J. Chem. Phys.* **87**(4), 2225–2230 (1987).
- ⁴⁹Y. Handa, O. Mishima, and E. Whalley, *J. Chem. Phys.* **84**(5), 2766–2770 (1986).
- ⁵⁰M. A. Floriano, Y. P. Handa, D. D. Klug, and E. Whalley, *J. Chem. Phys.* **91**(11), 7187–7192 (1989).
- ⁵¹O. Mishima and Y. Suzuki, *Nature* **419**(6907), 599 (2002).
- ⁵²O. Mishima, K. Takemura, and K. Aoki, *Science* **254**(5030), 406 (1991).
- ⁵³D. Klug, O. Mishima, and E. Whalley, *J. Chem. Phys.* **86**(10), 5323–5328 (1987).
- ⁵⁴O. Stal’gorova, E. Gromnitskaya, V. Brazhkin, and A. Lyapin, *JETP Lett.* **69**(9), 694–700 (1999).
- ⁵⁵E. L. Gromnitskaya, O. Stal’gorova, A. G. Lyapin, V. V. Brazhkin, and O. Tarutin, *JETP Lett.* **78**(8), 488–492 (2003).
- ⁵⁶E. L. Gromnitskaya, O. V. Stal’gorova, V. V. Brazhkin, and A. G. Lyapin, *Phys. Rev. B* **64**(9), 094205 (2001).
- ⁵⁷M. M. Koza, R. P. May, and H. Schober, *J. Appl. Crystallogr.* **40**(s1), s517–s521 (2007).
- ⁵⁸C. Kim, B. Barstow, M. W. Tate, and S. M. Gruner, *Proc. Natl. Acad. Sci. U. S. A.* **106**(12), 4596–4600 (2009).
- ⁵⁹J. Bachler, V. Fuentes-Landete, D. A. Jahn, J. Wong, N. Giovambattista, and T. Loerting, *Phys. Chem. Chem. Phys.* **18**(16), 11058–11068 (2016).
- ⁶⁰O. Mishima, *J. Chem. Phys.* **126**(24), 244507 (2007).
- ⁶¹Y. Suzuki, *J. Chem. Phys.* **147**(6), 064511 (2017).
- ⁶²Y. Suzuki and O. Mishima, *J. Chem. Phys.* **138**(8), 084507 (2013).
- ⁶³Y. Suzuki and O. Mishima, *J. Chem. Phys.* **141**(9), 094505 (2014).
- ⁶⁴Y. Suzuki and O. Mishima, *J. Chem. Phys.* **145**(2), 024501 (2016).
- ⁶⁵Z. Zhao and C. A. Angell, *Angew. Chem., Int. Ed.* **55**(7), 2474–2477 (2016).
- ⁶⁶G. P. Johari and O. Andersson, *J. Chem. Phys.* **120**(13), 6207–6213 (2004).
- ⁶⁷M. Guthrie, J. Urquidi, C. A. Tulk, C. J. Benmore, D. D. Klug, and J. Neufeind, *Phys. Rev. B* **68**(18), 184110 (2003).
- ⁶⁸J. S. Tse, D. D. Klug, M. Guthrie, C. A. Tulk, C. J. Benmore, and J. Urquidi, *Phys. Rev. B* **71**(21), 214107 (2005).
- ⁶⁹C. A. Tulk, C. J. Benmore, J. Urquidi, D. D. Klug, J. Neufeind, B. Tomberli, and P. A. Engelstaff, *Science* **297**(5585), 1320–1323 (2002).
- ⁷⁰M. Koza, T. Hansen, R. P. May, and H. Schober, *J. Non-Cryst. Solids* **352**(42–49), 4988–4993 (2006).
- ⁷¹M. M. Koza, B. Geil, K. Winkel, C. Köhler, F. Czeschka, M. Scheuermann, H. Schober, and T. Hansen, *Phys. Rev. Lett.* **94**(12), 125506 (2005).
- ⁷²M. Scheuermann, B. Geil, K. Winkel, and F. Fujara, *J. Chem. Phys.* **124**(22), 224503 (2006).
- ⁷³T. Loerting, K. Winkel, M. Seidl, M. Bauer, C. Mitterdorfer, P. H. Handle, C. G. Salzmänn, E. Mayer, J. L. Finney, and D. T. Bowron, *Phys. Chem. Chem. Phys.* **13**(19), 8783–8794 (2011).
- ⁷⁴K. Winkel, M. Bauer, E. Mayer, M. Seidl, M. S. Elsaesser, and T. Loerting, *J. Phys.: Condens. Matter* **20**(49), 494212 (2008).
- ⁷⁵P. H. Handle and T. Loerting, *Phys. Chem. Chem. Phys.* **17**(7), 5403–5412 (2015).
- ⁷⁶P. H. Handle and T. Loerting, *Phys. Rev. B* **93**(6), 064204 (2016).
- ⁷⁷M. S. Elsaesser, I. Kohl, E. Mayer, and T. Loerting, *J. Phys. Chem. B* **111**(28), 8038–8044 (2007).
- ⁷⁸K. Winkel, W. Schustereder, I. Kohl, C. G. Salzmänn, E. Mayer, and T. Loerting, in *Physics and Chemistry of Ice*, Special Publications, edited by W. Kuhs (The Royal Society of Chemistry, 2007), pp. 641–648.
- ⁷⁹M. Bauer, M. S. Elsaesser, K. Winkel, E. Mayer, and T. Loerting, *Phys. Rev. B* **77**(22), 220105 (2008).
- ⁸⁰P. H. Handle, M. Seidl, V. Fuentes-Landete, and T. Loerting, *Thermochim. Acta* **636**, 11–22 (2016).
- ⁸¹C. G. Salzmänn, E. Mayer, and A. Hallbrucker, *Phys. Chem. Chem. Phys.* **6**(22), 5156–5165 (2004).
- ⁸²M. Seidl, K. Amann-Winkel, P. H. Handle, G. Zifferer, and T. Loerting, *Phys. Rev. B* **88**(17), 174105 (2013).
- ⁸³M. Seidl, A. Fayer, J. N. Stern, G. Zifferer, and T. Loerting, *Phys. Rev. B* **91**(14), 144201 (2015).
- ⁸⁴P. H. Handle, “Relaxationsdynamik in hochdichtem amorphem Eis,” M.Sc. thesis, Universität Innsbruck, 2010.

- ⁸⁵Y. Suzuki and Y. Tominaga, *J. Chem. Phys.* **133**(16), 164508 (2010).
- ⁸⁶O. Mishima, *J. Chem. Phys.* **121**(7), 3161–3164 (2004).
- ⁸⁷M. Seidl, M. S. Elsaesser, K. Winkel, G. Zifferer, E. Mayer, and T. Loerting, *Phys. Rev. B* **83**(10), 100201 (2011).
- ⁸⁸N. Giovambattista, F. Sciortino, F. W. Starr, and P. H. Poole, *J. Chem. Phys.* **145**(22), 224501 (2016).
- ⁸⁹N. Giovambattista, F. W. Starr, and P. H. Poole, *J. Chem. Phys.* **147**(4), 044501 (2017).
- ⁹⁰V. F. Petrenko and R. W. Whitworth, *Physics of Ice* (Oxford University Press, 1999).
- ⁹¹H. E. Swanson and E. Tatge, *Standard X-ray Diffraction Powder Patterns, Volume I of National Bureau of Standards Circular* (U.S. Dept. of Commerce, National Bureau of Standards, 1953).